

Swarthmore College

Works

Chemistry & Biochemistry Faculty Works

Chemistry & Biochemistry

3-15-1989

The Spectroscopy And A State Dynamics Of The NeI Br Van Der Waals Complex

William Robert Simpson , '88

Thomas Alex Stephenson
Swarthmore College, tstephe1@swarthmore.edu

Follow this and additional works at: <https://works.swarthmore.edu/fac-chemistry>

 Part of the [Physical Chemistry Commons](#)

Let us know how access to these works benefits you

Recommended Citation

William Robert Simpson , '88 and Thomas Alex Stephenson. (1989). "The Spectroscopy And A State Dynamics Of The NeI Br Van Der Waals Complex". *Journal Of Chemical Physics*. Volume 90, Issue 6. 3171-3180. DOI: 10.1063/1.455867
<https://works.swarthmore.edu/fac-chemistry/5>

This work is brought to you for free by Swarthmore College Libraries' Works. It has been accepted for inclusion in Chemistry & Biochemistry Faculty Works by an authorized administrator of Works. For more information, please contact myworks@swarthmore.edu.

The spectroscopy and A state dynamics of the NiBr van der Waals complex

William R. Simpson and Thomas A. Stephenson

Citation: *The Journal of Chemical Physics* **90**, 3171 (1989); doi: 10.1063/1.455867

View online: <http://dx.doi.org/10.1063/1.455867>

View Table of Contents: <http://scitation.aip.org/content/aip/journal/jcp/90/6?ver=pdfcov>

Published by the AIP Publishing



Re-register for Table of Content Alerts

Create a profile.



Sign up today!



The spectroscopy and *A* state dynamics of the NeIBr van der Waals complex

William R. Simpson and Thomas A. Stephenson^{a)}

Department of Chemistry, Swarthmore College, Swarthmore, Pennsylvania 19081

(Received 20 September 1988; accepted 22 November 1988)

The $A\ ^3\Pi_1 \leftarrow X\ ^1\Sigma^+$ laser-induced fluorescence excitation spectrum of the NeIBr van der Waals complex is reported and analyzed to extract information regarding the structure and vibrational predissociation dynamics of the complex. While no definitive geometric information regarding NeIBr is obtained, our data indicate that a linear geometry is at least plausible. The vibrational predissociation lifetimes are a strong function of *A* state vibrational level and range from 2.6 to 23 ps. The variation in lifetime with vibrational level is consistent with the results of previous measurements on rare gas-halogen complexes, particularly NeBr₂.

I. INTRODUCTION

Investigations of the structure and dynamics of van der Waals complexes have provided valuable insights into long range potential interactions,¹ intramolecular dynamics,¹ and scattering phenomena from initial constrained geometries.^{2,3} Of the experimental studies of van der Waals molecules in excited electronic states, the most extensive have been those concerned with complexes composed of rare gas atoms and the diatomic halogens I₂,⁴⁻¹² Br₂,¹³⁻¹⁶ and Cl₂.¹⁷⁻²⁴ These experiments have focused on measurements of the binding energy, structure, and vibrational predissociation dynamics of the complexes in the $X\ ^1\Sigma_g^+$ and $B\ ^3\Pi_{0u}^+$ electronic states. The analogous heteronuclear interhalogen systems have received little attention to date, however. Klemperer and co-workers measured the electric resonance spectra of the ArClF²⁵ and KrClF²⁶ complexes and found that they are nearly linear. This result has proved to be at variance with geometric studies of the rare gas complexes of the homonuclear halogens, all of which assume a T-shaped geometry. Lester and co-workers have examined in great detail the structure and vibrational predissociation dynamics of the NeICl²⁷⁻³¹ and HeICl^{3,27,32,33} complexes upon excitation to the $A\ ^3\Pi_1$ and $B\ ^3\Pi_0^+$ electronic states. Like the homonuclear halogen complexes, HeICl is found to be nearly T-shaped in the *X* and *B* electronic states.³³ These workers also find that a nonlinear geometry is consistent with the ICl product rotational distributions that result from vibrational predissociation of HeICl and that these distributions reflect the anisotropy of the He/ICl potential energy surface.³ Their data do not reveal a definitive structure for the NeICl complex.

The interhalogen iodine monobromide, IBr, is an attractive species for use in studies of rare gas-interhalogen van der Waals complexes for several reasons. IBr has a molecular dipole moment that is nearly the same as that of ClF, but is much more polarizable, presenting some opportunity to explore the rationale for the anomalous structures of the van der Waals complexes containing ClF. The rare gas-I₂ and rare gas-Br₂ complexes are among the best characterized; comparison with these data should provide new insights into

the importance of the electronic and vibrational properties of the uncomplexed molecule on the vibrational predissociation dynamics of van der Waals complexes. Finally, as first documented by Brown³⁴ and examined in great detail by Selin and Söderborg,³⁵⁻³⁷ IBr has rich visible and near-infrared electronic spectroscopy. Excitation to three different adiabatic electronic states [$A\ ^3\Pi_1$, $B\ ^3\Pi_0^+$, and $B'(0^+)$] is possible using commercial YAG pumped dye lasers. Our new findings with respect to the $B \leftarrow X$ ³⁸ and $A \leftarrow X$ ³⁹ laser-induced fluorescence excitation spectra of uncomplexed, jet-cooled IBr will be presented elsewhere along with a discussion of our inability to observe rare gas-IBr complexes associated with the *B* electronic state. In this paper, we report the results of our study of the $A\ ^3\Pi_1 \leftarrow X\ ^1\Sigma^+$ spectroscopy and *A* state predissociation dynamics of the NeIBr van der Waals complex.

II. EXPERIMENTAL

NeIBr van der Waals complexes are formed in the supersonic free jet expansion of a mixture of IBr vapor with helium and neon. The expansion source is a pulsed solenoid valve (General Valve) with an orifice diameter of 150 μm . Our vacuum chamber is a welded stainless steel six way "cross" with a volume of ≈ 13 ℓ and is evacuated by a 6 in. diffusion pump (CVC Goldline) equipped with a high vacuum valve and freon cooled baffle. The diffusion pump fore-line contains a removeable, liquid nitrogen cooled glass trap to prevent corrosive halogen vapors from condensing in the mechanical forepump (Sargent-Welch 1397).

Excitation of the $A \leftarrow X$ transition in the IBr and NeIBr was accomplished using a commercial Nd³⁺-YAG pumped dye laser system (Quantel YG580-30/TDL-50) operating at 30 Hz. The excitation wavelength range of interest, 710-735 nm, is generated using LD 700 laser dye (Exciton). On the basis of spectral simulations, we estimate the excitation bandwidth (dye laser bandwidth plus Doppler broadening) to be 0.11 cm^{-1} FWHM. The dye laser wavelength drive was calibrated by recording Ne optogalvanic signals derived from an Fe/Ne hollow cathode lamp (Hamamatsu). The laser beam was mildly focused with a 1 m focal length lens to a spot ≈ 1 mm in diameter at the center of the chamber. In all

^{a)} Author to whom all correspondence should be addressed.

experiments the laser intersected the free jet expansion at a right angle 20 nozzle diameters downstream from the expansion source. The wavelength drive of dye laser was controlled using a PC-AT compatible computer (PC's Limited 286-8) using the RS-232 interface supplied by the laser manufacturer.

Fluorescence was detected perpendicular to both the central axis of the free jet expansion and the propagation axis of laser. Light was collected using a dual lens, $f/1.18$ optical system with an overall magnification of -1.0 . A red pass colored glass filter (Schott RG-780) was inserted in front of the photomultiplier (Thorn/EMI 9816B) to minimize the effects of scattered excitation laser light. The fluorescence photomultiplier output was routed to a preamplifier (EG&G Ortec 9305) and then to the input of a gated integrator (Stanford Research Systems SR250). To correct the fluorescence intensities for shot-to-shot variation in the laser energy, a fraction of the excitation beam was picked off with a glass microscope slide and was detected by a second photomultiplier (Hamamatsu R446) after passing through appropriate neutral density filters and a diffuser plate. The output of this photomultiplier was fed into a second gated integrator (Evans Associates 4130A). The output of both integrators was digitized with A/D converters (Stanford Research Systems SR245 Computer Interface Module); the resulting data was transferred to the laboratory computer for real time signal averaging, laser energy normalization and graphics output.

We were able to detect the fluorescence excitation features associated with the NeIBr complex using a wide range of Ne/He carrier gas mixtures and expansion pressures. One serious complication became apparent very early in our work. The bandshift between the excitation features of IBr is nearly identical to the $I^{79}\text{Br}-I^{81}\text{Br}$ isotope shift for many of the vibronic transitions of interest. Thus, for a given value of v' the excitation features for the $\text{Ne}_1I^{81}\text{Br}$ complex and the $I^{79}\text{Br}$ uncomplexed molecule lie at very nearly the same frequency, while the $\text{Ne}_2I^{81}\text{Br}$ and $\text{Ne}_1I^{79}\text{Br}$ features are also overlapped. To carry out a clean study of the NeIBr complex, we were forced, therefore, to examine only the $\text{Ne}I^{79}\text{Br}$ complex and to operate the expansion under conditions such that the Ne_2IBr complexes were not formed in detectable quantities. Our choice of a 3% Ne, 97% He carrier gas mixture and a total backing pressure of 350 psig represents the optimal conditions for the formation of NeIBr without interference from Ne_2IBr . Except as noted, all spectra reported here were recorded using these conditions. Commercial samples of IBr (Aldrich), neon (Aircro, "first run" grade) and helium (MG Industries) were used without modification. Our IBr sample cylinder was held at room temperature.

III. RESULTS

In Fig. 1, we show the $A-X$ laser-induced fluorescence excitation spectrum of IBr in the vicinity of the (14,0) vibronic transition using 100% helium and 5% neon/95% helium carrier gas mixtures. [We use the standard (v',v'') notation throughout to denote the various vibronic transitions.] Features due to the NeIBr and Ne_2IBr van der Waals

complex are clearly visible in Fig. 1(b). The shift of the excitation features due to both complexes to higher frequencies indicates that the complex is less strongly bound in the excited electronic state than in the ground state, a universal feature of the halogen and interhalogen/rare gas complexes studied to date.^{4,10,11,13,14,17,18,23,27} In Fig. 2, the NeIBr-to-IBr bandshifts are displayed as a function of v' , with the also common result that the band shift increases with v' ; the immediate conclusion is that the binding energy of the rare gas atom decreases with increasing vibrational excitation in the excited electronic state. For a particular value of v' , we find that the excitation shift of Ne_2IBr from NeIBr is nearly the same as the shift of NeIBr from uncomplexed IBr. For the (14,0) transitions, these values are 5.9 and 5.8 cm^{-1} , respectively. Thus, as in all other rare gas/halogen or interhalogen systems, the now common "band shift rule" is apparently obeyed in the Ne/IBr system for small numbers of attached neon atoms.

In Fig. 3, we show the laser-induced fluorescence excitation spectra of the (13,0) transition of $I^{79}\text{Br}$ along with our spectral simulation of this contour. By comparing the simulated and experimental spectra, we conclude that the excitation bandwidth is 0.11 cm^{-1} FWHM and that the IBr rotational temperature is 0.9 K . The detailed line shape of the (13,0) NeIBr excitation feature is displayed in Fig. 4(a). This feature, as with all other NeIBr transitions observed, is nearly symmetric and devoid of any recognizable rotational structure. It is also the narrowest NeIBr feature observed. [We have also recorded the (12,0) NeIBr excitation feature and find that, within our experimental uncertainty, it is identical to that for (13,0). We base much of our discussion below on the latter because of its superior signal-to-noise ratio. We are unable to observe transitions with smaller values of v' because of decreasing IBr Franck-Condon factors and the limited near-infrared sensitivity of our photodetector]. In all we have recorded excitation spectra associated with the $v' = 12-15$ and $17-19$ states of $\text{Ne}I^{79}\text{Br}$. [The (16,0) $\text{Ne}I^{79}\text{Br}$ transition is obscured by the (21,1) "hot band" transition in $I^{79}\text{Br}$.]

We have carried out a series of simulations of the rotational contour expected for NeIBr for a variety of assumed geometries, using the (13,0) experimental spectrum as the point of comparison. In these spectral simulations we have adopted the I-Br bond lengths appropriate for the uncomplexed molecule while varying the angle formed between the axis connecting the neon atom with the center-of-mass of IBr and IBr molecular axis (θ) and the radial distance between the neon atom and the IBr center-of-mass (R) (see Fig. 5). While we have sampled a large range of values of R and θ , we will concentrate our discussion here on four geometries that, based on previous investigations, seem most probable. The structure for only three rare gas-interhalogen van der Waals molecules have been determined to date. ArClF^{25} and KrClF^{26} are found to have nearly linear structures ($\theta = 11.1^\circ$ and 10.1° , respectively) with Cl the central atom while HeClI^{33} exists as a bent molecule, with $\theta = 90^\circ$. All of the rare gas-homonuclear halogen van der Waals molecules examined to date have T-shaped geometries ($\theta = 90^\circ$ ^{5,13,15,18,19,23}); the presumed rationale for the latter

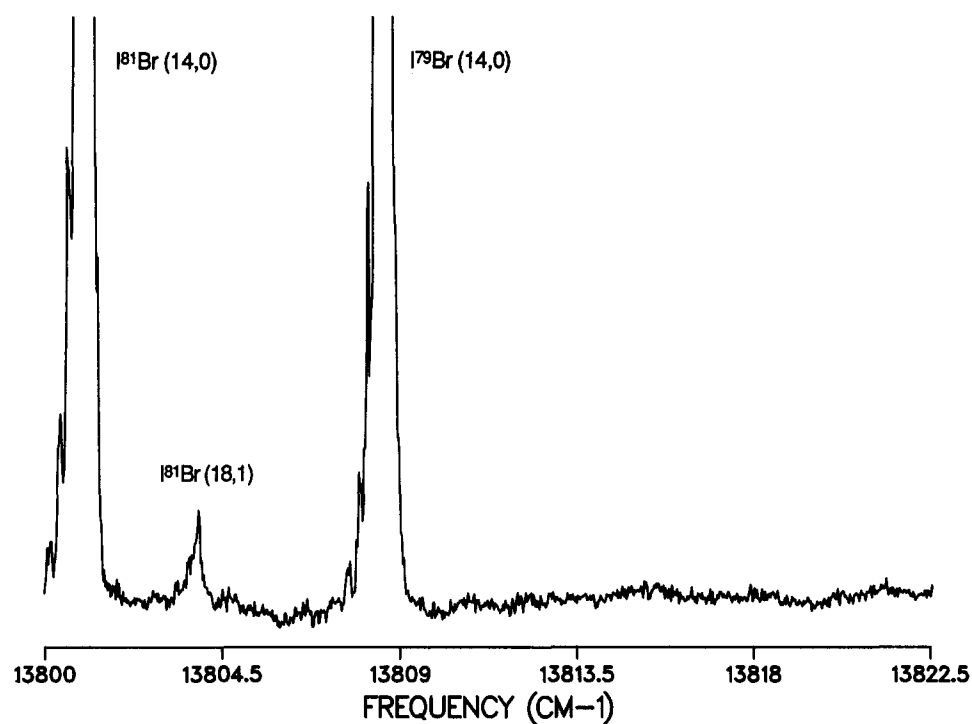
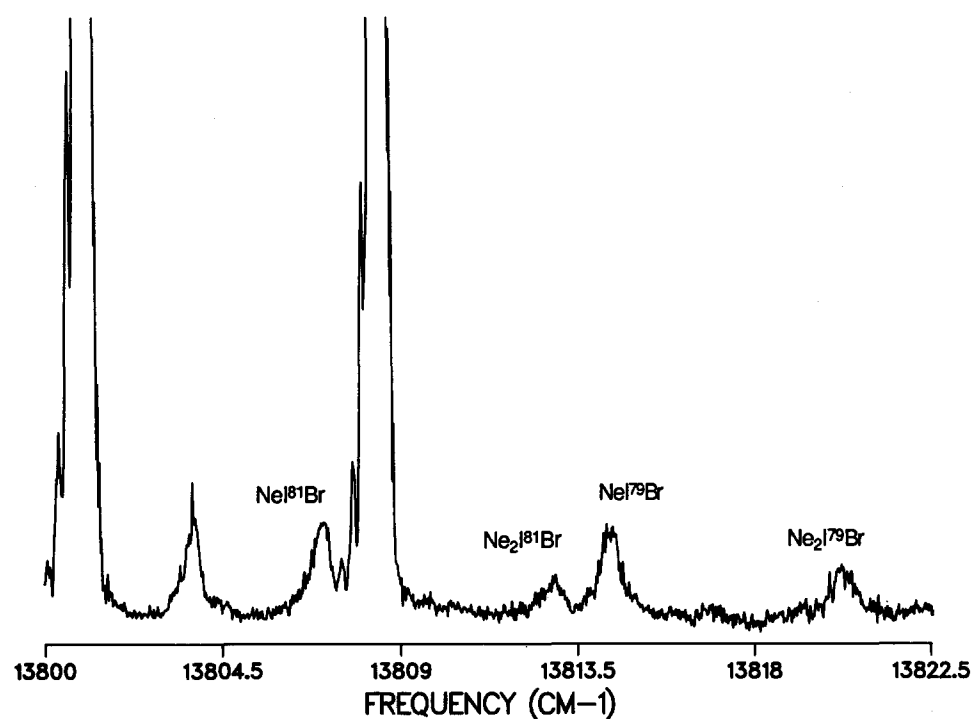


FIG. 1. $A \leftarrow X$ laser-induced fluorescence excitation spectra of IBr. (a) 100% helium carrier gas, 300 psig. (b) 5% neon/95% helium carrier gas; 300 psig.



observations is the optimization of the atom-atom pairwise interactions. This latter consideration suggests that the NeIBr complex, if it exists as a bent molecule, should have a "close-packed" structure with a value of θ that reflects the differences between the iodine and bromine van der Waals radii. A simple geometrical calculation suggests that, using this criterion for the structure of NeIBr, $\theta \approx 80^\circ$. We have, therefore, concentrated our efforts on structures with $\theta = 0^\circ$ (the central atom is bromine), 180° (the central atom is io-

dine), 80° , and in light of the finding of Skene regarding HeICl,³³ 90° . We note, however, that we have sampled several other nonlinear geometries ($\theta = 15^\circ, 30^\circ, 60^\circ$, and 70°) and find that the spectra resulting from these structures follow the general trends indicated in our discussion below.

Our choice of van der Waals bond lengths was also guided by the findings of previous investigations, in this case the structures of the NeBr₂¹⁵ and NeCl₂¹⁹ complexes. For both species, the Ne-X distance (X = Br, Cl) in the ground elec-

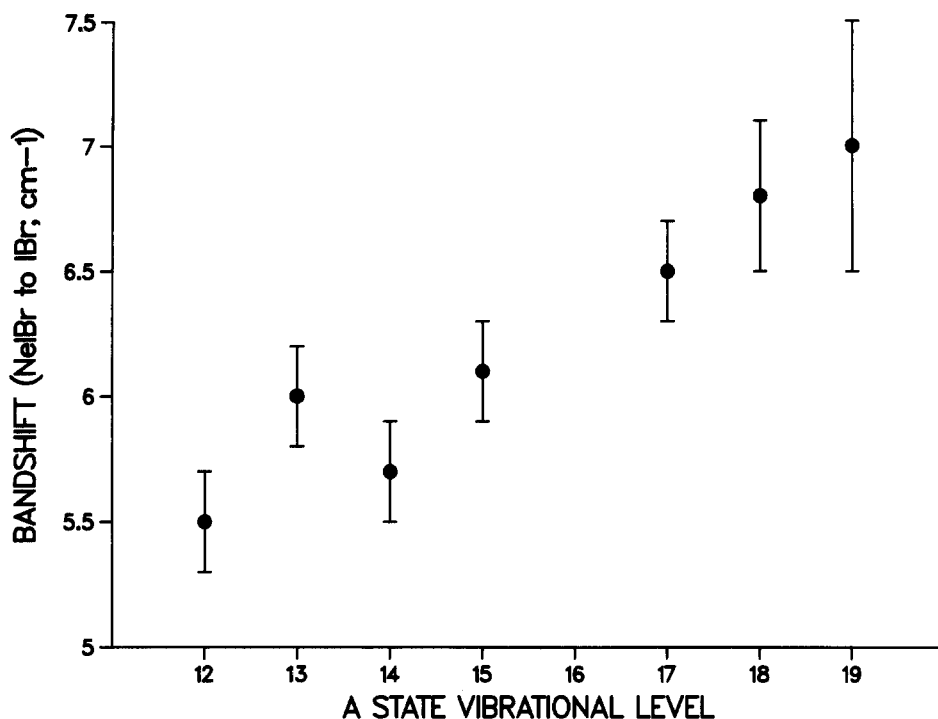


FIG. 2. IBBr-to-NeIBr excitation feature bandshifts as a function of *A* state vibrational level.

tronic state is found to be $\approx 0.3 \text{ \AA}$ larger than the sum of the relevant van der Waals radii and increases only slightly upon electronic excitation. Because of the significant increase in the diatomic halogen bond length upon excitation, the van der Waals bond length R is actually shorter in the *B* electronic state than in the ground state for both NeCl_2 and

NeBr_2 . By straightforward adoption of these principles, we estimate that, as a first approximation, the van der Waals bond length for a nonlinear NeIBr complex is $\approx 3.7 \text{ \AA}$ in the ground electronic state and $\approx 3.6 \text{ \AA}$ in the excited electronic state. All of the simulations pertaining to nonlinear geometries displayed here have assumed these bond lengths. We

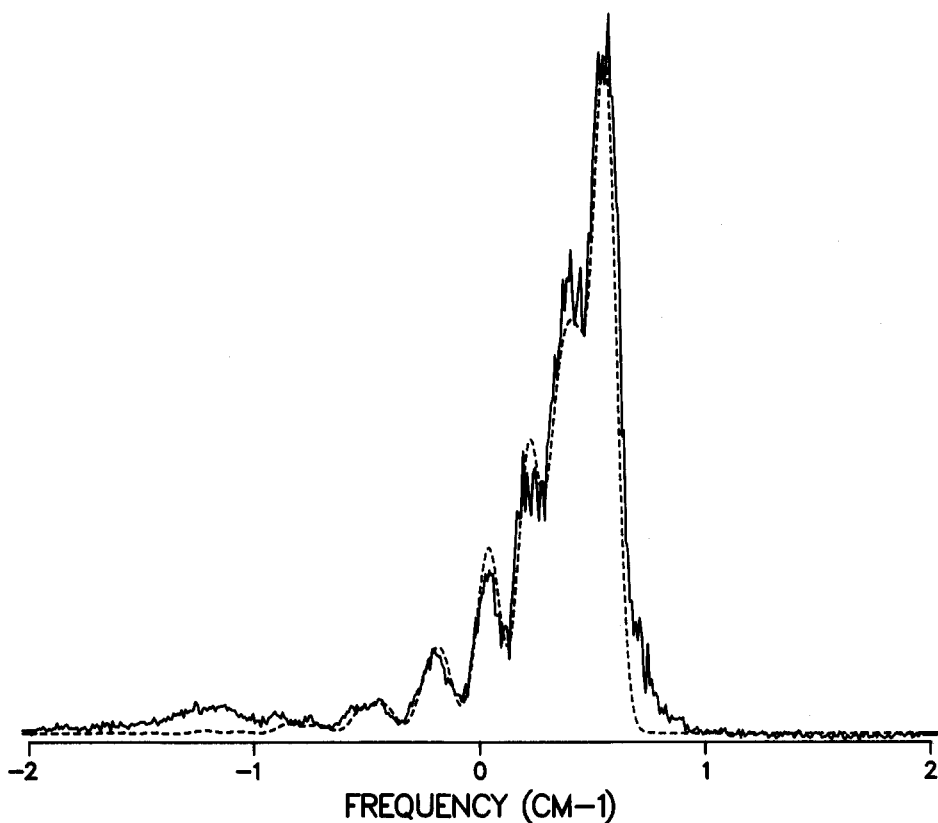


FIG. 3. $\text{I}^{79}\text{Br}(13,0)$ excitation spectrum: — experimental; --- simulation assuming $T_{\text{rot}} = 0.9 \text{ K}$ and an excitation bandwidth of 0.11 cm^{-1} FWHM. The rotational constants are adopted from Refs. 35 and 40. The broad, weak feature to lower frequency is the $(13,0)$ transition in NeI^{81}Br .

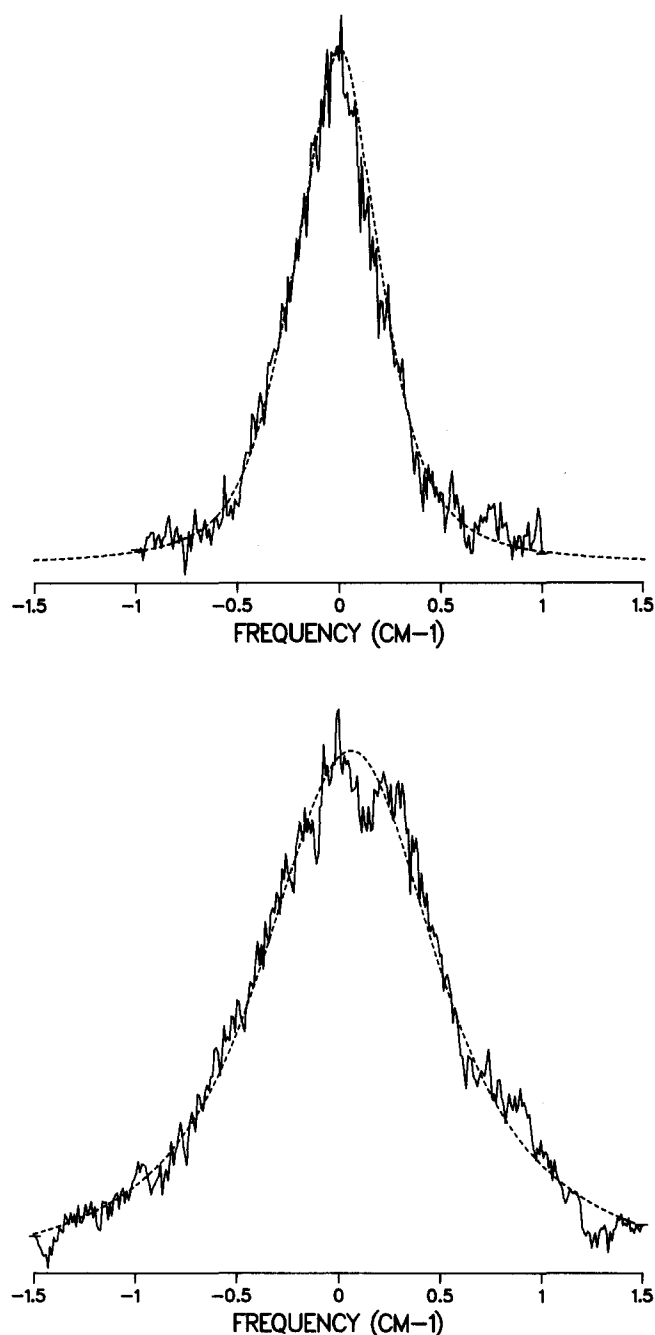


FIG. 4. NeIBr excitation spectra. (a) (13,0) transition: — experimental spectrum; --- simulation assuming $\theta = 80^\circ$, $T_{\text{rot}} = 0.2$ K, in-plane transition moment, Lorentzian width = 0.25 cm^{-1} . (b) (18,0) transition: — experimental spectrum; --- simulation assuming same parameters as in (a) except Lorentzian width = 0.90 cm^{-1} .

have, however, sampled X state bond lengths ranging from 3.5 to 4.1 Å and have considered changes upon excitation that range from -0.3 to $+0.2$ Å without any significant deviations from the trends discussed below.

We find that the simulations assuming a linear geometry for the complex are insensitive to the values of R'' and R' (the relative positions of the Ne atom and the IBr center of mass in the ground and excited electronic states, respectively). For the simulations presented here, we assume that the

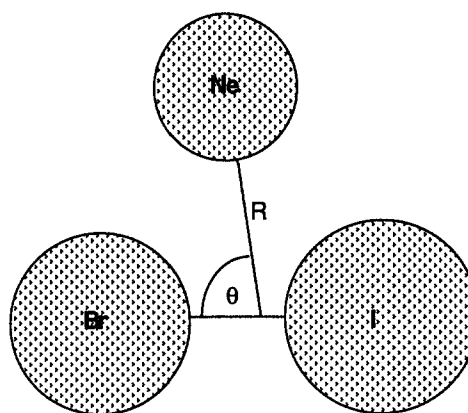


FIG. 5. Coordinates used to define NeIBr geometry.

Ne-Br ($\theta = 0^\circ$) and Ne-I ($\theta = 180^\circ$) distances are approximately the sum of the relevant van der Waals radii. In this case, $R'' = 5.0$ Å and $R' = 5.5$ Å for $\theta = 0^\circ$; $R'' = 4.6$ Å and $R' = 4.9$ Å when $\theta = 180^\circ$. These parameters yield spectra that are representative of a wide range of R' and R'' values.

A remaining variable in our spectral simulations is the choice of selection rules. The rare gas-halogen van der Waals complex features studied to date using rotational contour analysis have all involved excitation of the $B(\Omega = 0)$ state of the halogen (using Hund's case c notation) from the $\Omega = 0$ ground state. Thus the transition moment for all such excitations lies parallel to the diatomic halogen bond and in the molecular plane of the van der Waals complex. The selection rules for such transitions are determined simply from the degree to which the A inertial axis of the complex lies parallel to the bond of the diatomic halogen. For the $\Delta\Omega = +1 A \leftarrow X$ transition in IBr, however, the transition moment is perpendicular to the IBr bond. Thus, in a nonlinear NeIBr complex the transition moment may lie in the plane or out of the plane of the molecule (corresponding to excitation to A' and A'' electronic states, respectively, in the relevant C_s symmetry point group). One might in principle, therefore, observe two excitation features for the NeIBr complex ($A' \leftarrow A'$, $A'' \leftarrow A'$), corresponding to excited electronic states that lie at different energies. Since in a planar molecule the C inertial axis must lie perpendicular to the molecular plane, the out-of-plane polarized transitions must obey C -type selection rules, while the in-plane polarized transition will obey A - or B -type selection rules. An additional complicating feature of the NeIBr system is that the mass of neon is sufficient to cause a significant change in the directions of the inertial axes (assuming a nonlinear geometry) from those trivially derived for uncomplexed IBr. Thus for values of $\theta \neq 90^\circ$, the in-plane transitions are hybrid A -, B -type bands. As discussed below, we have considered both in-plane and out-of-plane rotational selection rules in our simulations involving nonlinear geometries. Clearly for a complex with a linear geometry these considerations are moot, as the in-plane and out-of-plane transition moments become spatially degenerate when $\theta = 0^\circ$ or 180° .

In Fig. 6, the simulations corresponding to the four structures described in the preceding paragraphs are dis-

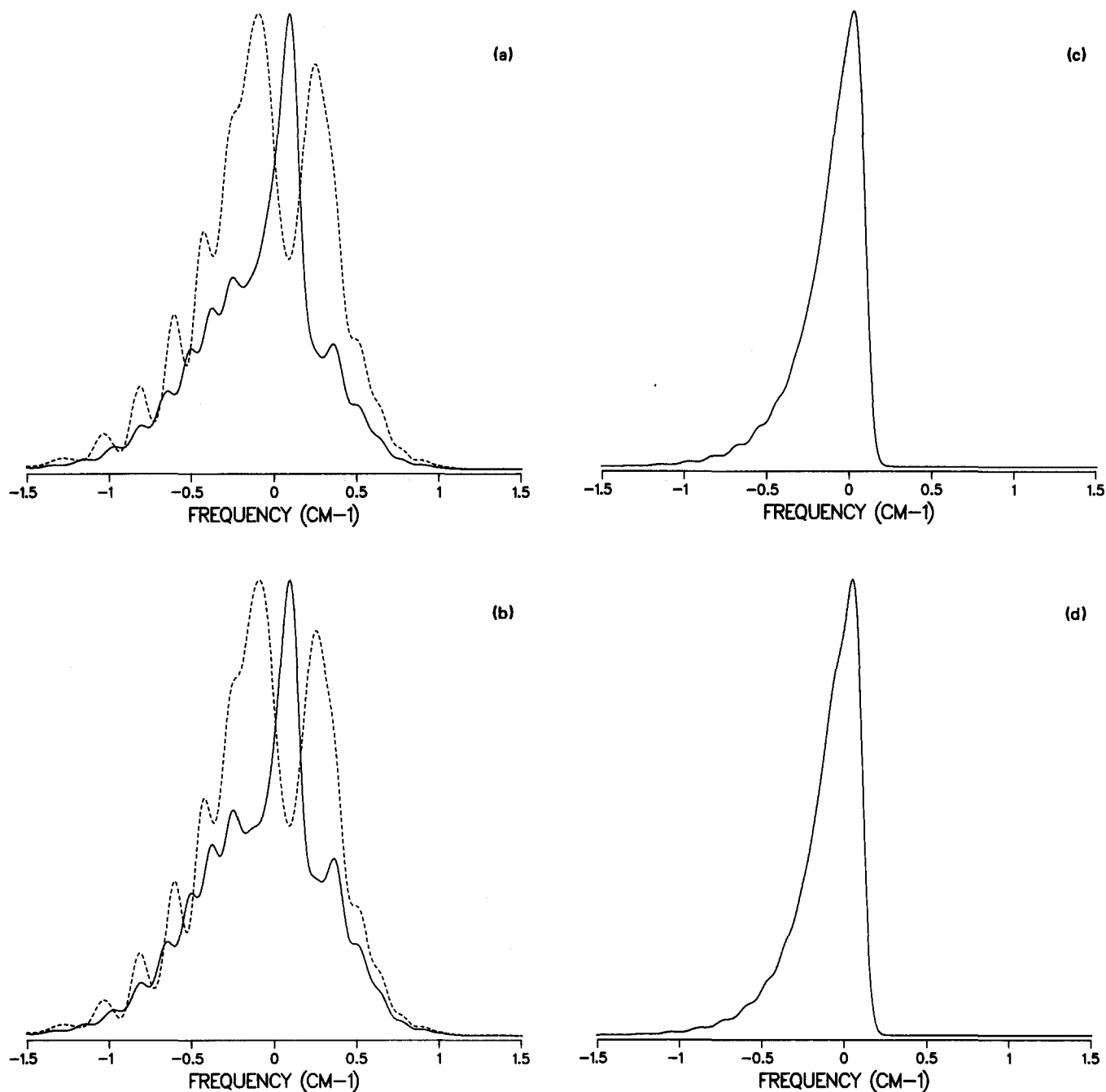


FIG. 6. Simulated NeIBr spectra; $T_{\text{rot}} = 0.9$ K; assuming no homogeneous broadening. (a) $\theta = 80^\circ$: — in-plane transition moment; --- out-of-plane transition moment. (b) $\theta = 90^\circ$: — in-plane transition moment; --- out-of-plane transition moment. (c) $\theta = 0^\circ$. (d) $\theta = 180^\circ$.

played. In all cases, the excitation bandwidth (0.11 cm^{-1}) and rotational temperature (0.9 K) from our uncomplexed IBr spectra have been assumed. For the nonlinear geometries, the spectra obtained from hybrid *A*-, *B*- (in-plane transition moment) and *C*- (out-of-plane transition moment) type selection rules are displayed on the same axes. A comparison with our experimental (13,0) spectrum reveals several important general findings. First, in the absence of lifetime broadening, the nonlinear geometries give rise to the identifiable rotational structure at our level of excitation res-

olution that is not observed experimentally. Second, the spectra derived from using *C*-type (out-of-plane transition moment) selection rules are in general too broad to be a reasonable match for the experimental spectra. Third, the spectra derived from the linear geometries are sufficiently narrow to suggest that lifetime broadening must play a role in the experimental spectra, but they display a degree of asymmetry that is not reproduced experimentally. We have convoluted the spectra shown in Fig. 6 with Lorentzian line shapes of various widths with the result that *for all geome-*

tries we are unable to match both the striking symmetry of the (13,0) experimental spectrum and its relatively narrow bandwidth. To fit the experimental spectra, we have found it necessary to relax the assumption that the rotational temperature of the complex is the same as that of uncomplexed IBr. When we vary both the applied Lorentzian broadening and the rotational temperature, we are able to achieve a fit as indicated in Fig. 4(a). The remarkable result is that for all geometries, we find that Lorentzian widths in the range of $0.25\text{--}0.30\text{ cm}^{-1}$ are required to fit the experimental data. (The simulated spectra displayed in Fig. 4 are those for $\theta = 80^\circ$; identical fits are obtained for other values of θ). The rotational temperature needed to achieve a fit does, however, vary with the assumed geometry. The fit displayed in Fig. 4(a) is achieved only if the assumed rotational temperature is 0.2 K. Further, we note that only hybrid *A*-, *B*-type (in-plane selection rules) bands are an adequate match to the experimental data under these conditions. With temperatures as low as 0.2 K and Lorentzian widths chosen to reproduce the FWHM of the experimental feature, we find that rotational contours derived from type *C* selection rules [Fig. 7(a)] or a blend of type *C* and hybrid *A*, *B* selection rules have simply the wrong overall shape to represent the data. Either linear geometry is found to be consistent with the data when a rotational temperature of 0.6 K is assumed.

In our fitting procedure, we have focused on two key aspects of the (13,0) NeI Br excitation spectrum—its symmetry and width. Considering the hybrid *A*-, *B*-type band when $\theta = 80^\circ$ as an example, we find that values of T_{rot} higher than 0.2 K and applied Lorentzian widths of smaller than 0.25 cm^{-1} reproduce the FWHM of the feature, but result in contours that are asymmetric [Fig. 7(b)]. For $T_{\text{rot}} > 0.2\text{ K}$, a symmetric line shape is derived only by applying a Lorentzian line shape that is so broad (typically $\geq 0.50\text{ cm}^{-1}$ FWHM) that the FWHM of the experimental feature is exceeded. Similar considerations apply to our simulations which assume other nonlinear geometries or a linear geometry with $T_{\text{rot}} > 0.6\text{ K}$ [Fig. 7(c)]. Our assignment of a broadening of $0.25\text{--}0.30\text{ cm}^{-1}$ FWHM and a rotational temperature of 0.2 K (for a nonlinear geometry; $T_{\text{rot}} = 0.6\text{ K}$ for a linear geometry) represents the least extreme set of parameters required to match both the symmetry and width of the NeI Br feature. An equally good fit is achieved by assuming a lower rotational temperature and larger degree of lifetime broadening.

We have adjusted the Lorentzian widths added to our simulations to match the breadth of the NeI Br features with $v' \neq 13$ using as a starting point our best fit simulation to the (13,0) transition. (We have examined the effect of the variation of the I–Br equilibrium bond length with *A* state vibrational level on our simulations; the results described here are insensitive to such changes.) The result of this procedure is shown in Fig. 4(b) for the NeI Br (18,0) transition. In Fig. 8 and Table I, we present the results of our vibrational predissociation lifetime calculations, where the lifetimes (τ) have been calculated using the relation,⁴¹

$$\tau = (2\pi cW)^{-1}.$$

W is the applied Lorentzian broadening (FWHM) in wave

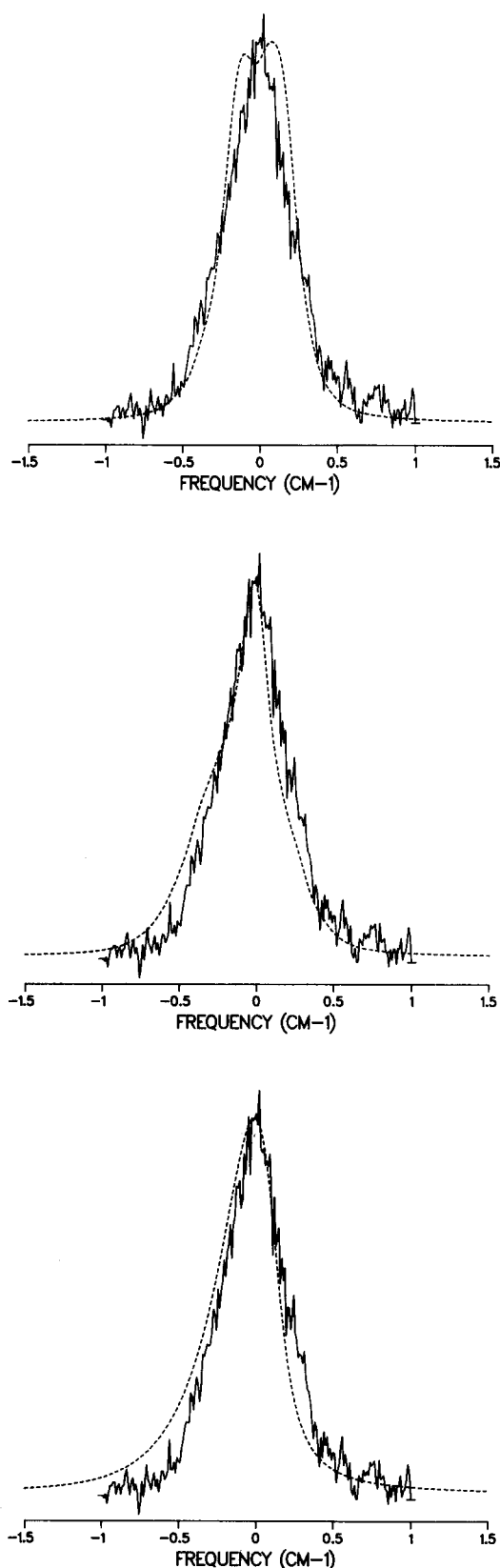


FIG. 7. Examples of geometric models deviating from the experimental spectra (see the text). — NeI Br (13,0) experimental spectrum; --- simulations assuming: (a) $\theta = 80^\circ$, $T_{\text{rot}} = 0.2\text{ K}$, *C*-type (out-of-plane transition moment) selection rules, Lorentzian width = 0.10 cm^{-1} ; (b) $\theta = 80^\circ$, $T_{\text{rot}} = 0.4\text{ K}$, *A*, *B*-type (in-plane transition moment) selection rules, Lorentzian width = 0.10 cm^{-1} ; (c) $\theta = 180^\circ$, $T_{\text{rot}} = 0.9\text{ K}$, Lorentzian width = 0.20 cm^{-1} .

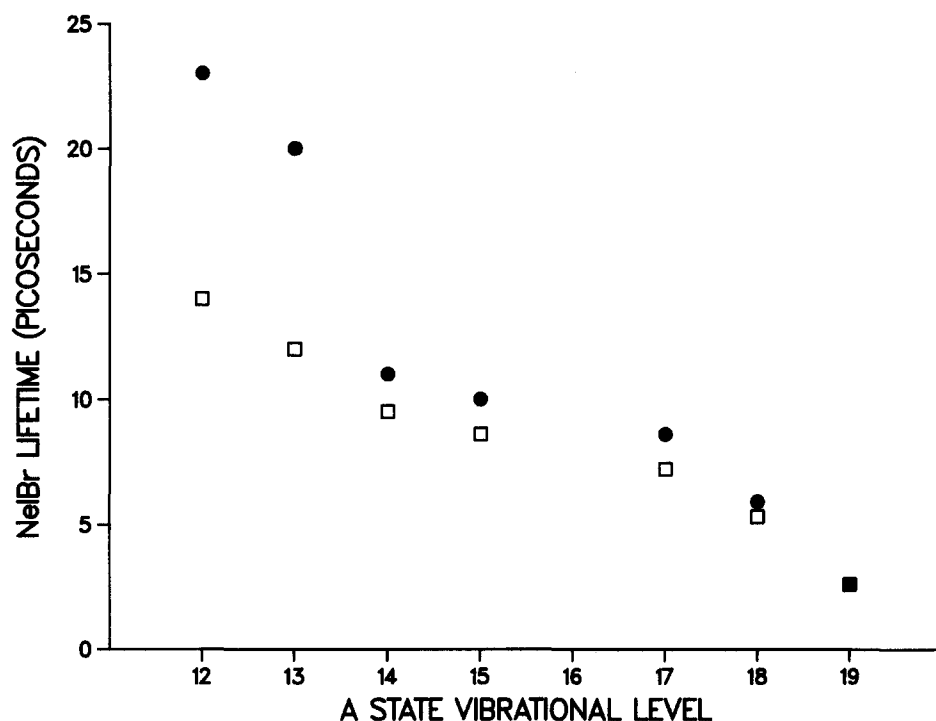


FIG. 8. NeI Br lifetime as a function of vibrational level. ● upper limit estimate; □ lower limit estimate. Error bars are omitted for clarity (see Table I).

numbers and c is the speed of light. The experimental uncertainties indicated in Table I are simply estimates of the range of broadening parameters that provide adequate fits to the experimental data. In each case the calculated lifetime represents an upper limit since a smaller assumed rotational temperature results in a greater degree of lifetime broadening. A lower limit for each lifetime can be calculated by assigning the entire width of each excitation feature to lifetime broadening. The results of these calculations are also shown in Table I.

IV. DISCUSSION

While we are unable to make any unambiguous statements concerning the geometry of the NeI Br complex, our simulations indicate that a linear geometry is at least plausible. As noted earlier, the observation of only one excitation feature is counter to our expectations for a complex with a nonlinear geometry. In this case, one should observe both $A' \leftarrow A'$ and $A'' \leftarrow A'$ transitions. The energy difference expected between the A' and A'' excited electronic states

is highly uncertain, however. Calculations⁴² and experiments⁴³ carried out on the ArNO($^2\Pi_{1/2}$) system indicate that the difference in energy between the states with the partially filled NO π orbital oriented in-plane and out-of-plane of the van der Waals complex is $\approx 3 \text{ cm}^{-1}$. In diatomic van der Waals complexes composed of $L = 1$ (i.e., P state) metal and rare gas atoms, the difference in energy between the resulting Σ and Π molecular states (differing by the orientation of the metallic p orbital with respect to the molecular axis) is often hundreds of cm^{-1} .⁴⁴ We observe no unidentified excitation features within $\pm 20 \text{ cm}^{-1}$ of those already assigned to NeI Br. While the experimental and theoretical literature on this subject is sketchy, our general assumption is that the energy separation between the A' and A'' electronic states in NeI Br will be more like that observed in ArNO than in the metallic systems. The absence of a C -type selection rule, out-of-plane polarized rotational contour suggests that no formal distinction exists between the in-plane and out-of-plane polarized transitions, i.e., the molecule assumes a linear configuration. Alternative interpretations

TABLE I. NeI Br vibrational predissociation lifetimes.

ν'	Upper limit calculation		Lower limit calculation	
	Linewidth (fit) ^a	Lifetime (ps)	Linewidth (max.) ^a	Lifetime (ps)
12	0.23 ± 0.05	23 ± 7	0.38 ± 0.05	14 ± 2
13	0.27 ± 0.05	20 ± 4	0.43 ± 0.05	12 ± 2
14	0.47 ± 0.05	11 ± 2	0.56 ± 0.05	9.5 ± 1.0
15	0.52 ± 0.05	10 ± 1	0.62 ± 0.05	8.6 ± 0.8
17	0.62 ± 0.05	8.6 ± 0.7	0.74 ± 0.05	7.2 ± 0.5
18	0.90 ± 0.05	5.9 ± 0.4	1.00 ± 0.05	5.3 ± 0.3
19	2.05 ± 0.4	2.6 ± 0.6	2.01 ± 0.4	2.6 ± 0.6

^a Wave number units (cm^{-1}), FWHM.

that cannot be discarded at this time are that only one excitation feature is observed because of differences in either (1) electronic transition moments between the $A' \leftarrow A'$ and $A'' \leftarrow A'$ excitation transitions or (2) predissociation dynamics on the electronically excited A' and A'' molecular potential energy surfaces. Conventional wisdom regarding rare gas-halogen van der Waals molecules is that the rare gas atom contributes only a small perturbation to the electronic structure of the halogen component. If option (1) is to be accepted, then this critical assumption must be reevaluated. Unfortunately, our data shed no light on the possibility that the dynamics on the excited A' and A'' surfaces are sufficiently different to make NeIBr in the excited A'' electronic state unobservable by conventional fluorescence excitation spectroscopy.

Contradicting these considerations is our finding that the Ne/IBr system obeys a normal band shift rule. This result suggests that there are at least two approximately equivalent binding sites for Ne with IBr. While it is trivial to find such sites for a nonlinear atomic configuration, it is not clear that such sites exist for a linear geometry. We also note that the magnitude of the blue shift of the excitation features of the complex relative to those of uncomplexed IBr mimics the behavior of rare gas-halogen complexes known to assume T-shaped geometries.^{4,10,11,13,14,17,18,23,24} Variations in the band shift with vibrational excitation similar to those observed here also occur in virtually all of the documented T-shaped rare gas-halogen complexes.

The vibrational predissociation dynamics of NeIBr follow a pattern in accord with the "momentum gap"⁴⁵ or "energy gap"⁴⁶ laws, i.e., the lifetime of the excited complex decreases as the vibrational spacing in the uncomplexed molecule decreases. This decrease in lifetime is particularly dramatic in NeIBr as the lifetime changes by a factor of almost 10 as the spacing between adjacent vibrational levels varies from 97 cm^{-1} [$E(v' = 12) - E(v' = 11)$] to 73 cm^{-1} [$E(v' = 19) - E(v' = 18)$]. In the $B^3\Pi_{0u}^+$ state of the NeBr₂ vibrational predissociation lifetimes vary in approximately the same fashion for a range of vibrational levels ($v' = 19$ – 26) with spacings similar to those of $v' = 12$ – 19 in the A state of IBr.¹⁴ In the case of NeBr₂, the dramatic decrease in the lifetime is ascribed to an approach to resonance between the binding energy of the complex and the energy available in the $\Delta v = -1$ relaxation channel in Br₂.¹⁴ We note that the ground electronic state binding energy of NeBr₂ ($\approx 73 \text{ cm}^{-1}$)¹⁴ and NeI₂ ($\approx 74 \text{ cm}^{-1}$)⁹ are quite close to one another and expect that the binding energy of NeIBr will be similar. Thus once the IBr-to-NeIBr band shift is taken into account, we anticipate that the A state NeIBr binding energy will be $\approx 65 \text{ cm}^{-1}$. In this case the $\Delta v = -1$ relaxation channel will be energetically closed for $v' \geq 21$. We are unable to observe any NeIBr excitation features for $v' > 19$, however, presumably because extensive homogeneous broadening makes them indistinguishable from our baseline noise.

Our inability to observe high v' excitation features means that we cannot comment on whether the lifetime of the complex increases just beyond the closure of the $\Delta v = -1$ channel. In the limit of pure V \rightarrow T energy transfer

in the dissociation process, the energy and momentum gap models predict a decrease in the predissociation rate as the amount of energy that is deposited into relative translation of the fragments increases, i.e., at the point that only channels with $|\Delta v| > 1$ are energetically open. Such threshold behavior has been observed in the vibrational state dependence of the predissociation lifetimes in HeI₂¹² and NeBr₂.¹⁴ Complexes containing IBr, with its large reduced mass, should be equally good candidates for pure V \rightarrow T transfer as angular momentum constraints severely limit the amount of energy that can be deposited into fragment rotation. In the analogous NeICl complexes, however, Lester and co-workers have demonstrated the importance of rotational energy transfer and $\Delta v \neq -1$ dissociation pathways for vibrational levels where the $\Delta v = -1$ channel remains open.^{30,31} An understanding of the degree to which this latter result is an indication of a general breakdown of the V \rightarrow T models for the anisotropic interhalogen systems will await further study of the rare gas-IBr and other interhalogen complexes, with an emphasis on produce quantum state distributions. The results of our study—band shifts, rotational contours and predissociation lifetimes—demonstrate that van der Waals complexes containing IBr exhibit sufficient features that are distinct from and in common with analogous halogen and interhalogen systems to provide a subtle test of our understanding of the geometry and dynamics of these unique species.

ACKNOWLEDGMENTS

This research has been supported by grants from the Research Corporation and the Swarthmore College Faculty Research Fund. Acknowledgment is made to the Donors of The Petroleum Research Fund, administered by the American Chemical Society, for partial support of this research. We are grateful to Professor M. I. Lester for numerous helpful discussions and for sharing the results of her group's work prior to publication.

¹For reviews, see B. L. Blaney and G. E. Ewing, *Annu. Rev. Phys. Chem.* **27**, 553 (1976); D. H. Levy, *Adv. Chem. Phys.* **47**, 323 (1981); R. J. LeRoy and J. S. Carley, *ibid.* **42**, 353 (1980); K. C. Janda, *ibid.* **60**, 201 (1985); S. A. Rice, *J. Phys. Chem.* **90**, 3036 (1986).

²J. Rice, G. Hoffman, and C. Wittig, *J. Chem. Phys.* **88**, 2841 (1988), and references cited therein; C. Jouvet, M. Boivineau, M. C. Duval, and B. Soep, *J. Phys. Chem.* **91**, 5416 (1987).

³R. L. Waterland, J. M. Skene, and M. I. Lester, *J. Chem. Phys.* **89**, 7277 (1988).

⁴R. E. Smalley, D. H. Levy, and L. Wharton, *J. Chem. Phys.* **64**, 3266 (1976).

⁵R. E. Smalley, L. Wharton, and D. H. Levy, *J. Chem. Phys.* **68**, 671 (1978).

⁶G. Kubiak, P. S. H. Fitch, L. Wharton, and D. H. Levy, *J. Chem. Phys.* **68**, 4477 (1978).

⁷K. E. Johnson, L. Wharton, and D. H. Levy, *J. Chem. Phys.* **69**, 2719 (1978).

⁸W. Sharfin, K. E. Johnson, K. Wharton, and D. H. Levy, *J. Chem. Phys.* **71**, 1292 (1979).

⁹J. A. Blazy, B. M. DeKoven, T. D. Russell, and D. H. Levy, *J. Chem. Phys.* **72**, 2439 (1980).

- ¹⁰J. E. Kenny, K. E. Johnson, W. Sharfin, and D. H. Levy, *J. Chem. Phys.* **72**, 1109 (1980).
- ¹¹K. E. Johnson, W. Sharfin, and D. H. Levy, *J. Chem. Phys.* **74**, 163 (1981).
- ¹²W. Sharfin, P. Kroger, and S. C. Wallace, *Chem. Phys. Lett.* **85**, 81 (1982).
- ¹³L. J. van de Burgt, J.-P. Nicolai, and M. C. Heaven, *J. Chem. Phys.* **81**, 5514 (1984).
- ¹⁴B. A. Swartz, D. E. Brinza, C. M. Western, and K. C. Janda, *J. Phys. Chem.* **88**, 6272 (1984).
- ¹⁵F. Thommen, D. D. Evard, and K. C. Janda, *J. Chem. Phys.* **82**, 5295 (1985).
- ¹⁶N. Sivakumar, J. I. Cline, C. R. Bieler, and K. C. Janda, *Chem. Phys. Lett.* **147**, 561 (1988).
- ¹⁷D. E. Brinza, C. M. Western, D. D. Evard, F. Thommen, B. A. Swartz, and K. C. Janda, *J. Phys. Chem.* **88**, 2004 (1984).
- ¹⁸J. I. Cline, D. D. Evard, F. Thommen, and K. C. Janda, *J. Chem. Phys.* **84**, 1165 (1986).
- ¹⁹D. D. Evard, F. Thommen, and K. C. Janda, *J. Chem. Phys.* **84**, 3630 (1986).
- ²⁰J. I. Cline, N. Sivakumar, D. D. Evard, and K. C. Janda, *J. Chem. Phys.* **86**, 1636 (1987).
- ²¹J. I. Cline, N. Sivakumar, D. D. Evard, and K. C. Janda, *Phys. Rev. A* **36**, 1944 (1987).
- ²²D. D. Evard, F. Thommen, J. I. Cline, and K. C. Janda, *J. Phys. Chem.* **91**, 2508 (1987).
- ²³D. D. Evard, J. I. Cline, and K. C. Janda, *J. Chem. Phys.* **88**, 5433 (1988).
- ²⁴D. D. Evard, C. R. Bieler, J. I. Cline, N. Sivakumar, and K. C. Janda, *J. Chem. Phys.* **89**, 2929 (1988).
- ²⁵S. J. Harris, S. E. Novick, W. Klemperer, and W. E. Falconer, *J. Chem. Phys.* **61**, 193 (1974).
- ²⁶S. E. Novick, S. J. Harris, K. C. Janda, and W. Klemperer, *Can. J. Phys.* **53**, 2007 (1975).
- ²⁷J. M. Skene, J. C. Drobits, and M. I. Lester, *J. Chem. Phys.* **85**, 2329 (1986).
- ²⁸J. C. Drobits, J. M. Skene, and M. I. Lester, *J. Chem. Phys.* **84**, 2896 (1986).
- ²⁹J. C. Drobits and M. I. Lester, *J. Chem. Phys.* **86**, 1662 (1987).
- ³⁰J. C. Drobits and M. I. Lester, *J. Chem. Phys.* **88**, 120 (1988).
- ³¹J. C. Drobits and M. I. Lester, *J. Chem. Phys.* **89**, 4716 (1988).
- ³²J. M. Skene and M. I. Lester, *Chem. Phys. Lett.* **116**, 93 (1985).
- ³³J. M. Skene, Ph.D. thesis, University of Pennsylvania, 1988.
- ³⁴W. G. Brown, *Phys. Rev.* **42**, 355 (1932).
- ³⁵L.-E. Selin, *Ark. Fys.* **21**, 479 (1962).
- ³⁶L.-E. Selin and B. Söderborg, *Ark. Fys.* **21**, 515 (1962).
- ³⁷L.-E. Selin, *Ark. Fys.* **21**, 529 (1962).
- ³⁸T. A. Stephenson, W. R. Simpson, J. R. Wright, H. P. Schneider, J. W. Miller, and K. E. Schultz, *J. Phys. Chem.* (in press).
- ³⁹W. R. Simpson and T. A. Stephenson (to be published).
- ⁴⁰E. M. Weinstock and A. Preston, *J. Mol. Spectrosc.* **70**, 188 (1978).
- ⁴¹Assumes negligible broadening in the ground electronic state.
- ⁴²G. C. Nielson, G. A. Parker, and R. T. Pack, *J. Chem. Phys.* **66**, 1396 (1977).
- ⁴³P. D. A. Mills, C. M. Western, and B. J. Howard, *J. Phys. Chem.* **90**, 4961 (1986).
- ⁴⁴See, for example, K. Fuke, T. Saito, and K. Koya, *J. Chem. Phys.* **81**, 2591 (1984); W. P. Lapatovich, R. Ahmed-Bitar, P. E. Moskowitz, I. Renhorn, R. A. Gottscho, and D. E. Pritchard *ibid.* **73**, 5419 (1980); A. Kowalski, D. J. Funk, and W. H. Breckenridge, *Chem. Phys. Lett.* **121**, 217 (1985); K. Yamanouchi, S. Isagai, M. Okunishi, and S. Tsuchiya, *J. Chem. Phys.* **88**, 205 (1988).
- ⁴⁵G. E. Ewing, *J. Chem. Phys.* **71**, 3143 (1979); *J. Phys. Chem.* **91**, 4662 (1987).
- ⁴⁶J. A. Beswick and J. Jortner, *Adv. Chem. Phys.* **47**, 363 (1981).